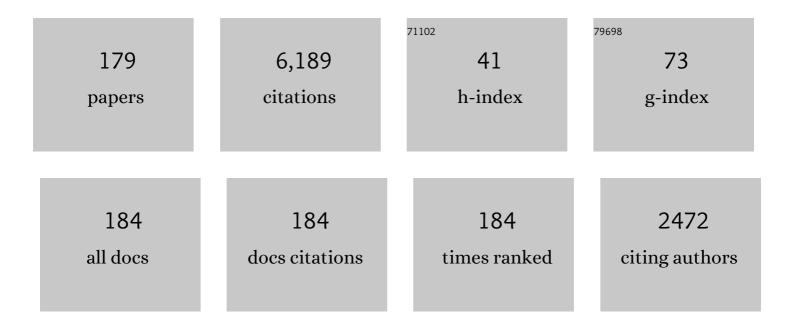
## Riccardo Tommasini

List of Publications by Year in descending order

Source: https://exaly.com/author-pdf/2907601/publications.pdf Version: 2024-02-01



#	Article	IF	CITATIONS
1	Fuel gain exceeding unity in an inertially confined fusion implosion. Nature, 2014, 506, 343-348.	27.8	742
2	Progress towards ignition on the National Ignition Facility. Physics of Plasmas, 2013, 20, .	1.9	259
3	Burning plasma achieved in inertial fusion. Nature, 2022, 601, 542-548.	27.8	233
4	Onset of Hydrodynamic Mix in High-Velocity, Highly Compressed Inertial Confinement Fusion Implosions. Physical Review Letters, 2013, 111, 085004.	7.8	215
5	Relativistic Quasimonoenergetic Positron Jets from Intense Laser-Solid Interactions. Physical Review Letters, 2010, 105, 015003.	7.8	161
6	The high-foot implosion campaign on the National Ignition Facility. Physics of Plasmas, 2014, 21, .	1.9	149
7	The experimental plan for cryogenic layered target implosions on the National Ignition Facility—The inertial confinement approach to fusion. Physics of Plasmas, 2011, 18, .	1.9	148
8	Inertially confined fusion plasmas dominated by alpha-particle self-heating. Nature Physics, 2016, 12, 800-806.	16.7	144
9	Implosion dynamics measurements at the National Ignition Facility. Physics of Plasmas, 2012, 19, .	1.9	125
10	High-density carbon ablator experiments on the National Ignition Facility. Physics of Plasmas, 2014, 21, .	1.9	116
11	High-resolution 17–75keV backlighters for high energy density experiments. Physics of Plasmas, 2008, 15, .	1.9	111
12	Demonstration of High Performance in Layered Deuterium-Tritium Capsule Implosions in Uranium Hohlraums at the National Ignition Facility. Physical Review Letters, 2015, 115, 055001.	7.8	101
13	Cryogenic thermonuclear fuel implosions on the National Ignition Facility. Physics of Plasmas, 2012, 19, .	1.9	95
14	Design of inertial fusion implosions reaching the burning plasma regime. Nature Physics, 2022, 18, 251-258.	16.7	87
15	Effect of the mounting membrane on shape in inertial confinement fusion implosions. Physics of Plasmas, 2015, 22, .	1.9	85
16	Development of nuclear diagnostics for the National Ignition Facility (invited). Review of Scientific Instruments, 2006, 77, 10E715.	1.3	84
17	Development of Compton radiography of inertial confinement fusion implosions. Physics of Plasmas, 2011, 18, .	1.9	82
18	of Diamon 2015, 22, 05(215	1.9	82

of Plasmas, 2015, 22, 056315.

1.9 82

#	Article	IF	CITATIONS
19	Dynamic symmetry of indirectly driven inertial confinement fusion capsules on the National Ignition Facility. Physics of Plasmas, 2014, 21, .	1.9	81
20	Reduced instability growth with high-adiabat high-foot implosions at the National Ignition Facility. Physical Review E, 2014, 90, 011102.	2.1	77
21	Record Energetics for an Inertial Fusion Implosion at NIF. Physical Review Letters, 2021, 126, 025001.	7.8	76
22	Nuclear imaging of the fuel assembly in ignition experiments. Physics of Plasmas, 2013, 20, 056320.	1.9	65
23	Indirect drive ignition at the National Ignition Facility. Plasma Physics and Controlled Fusion, 2017, 59, 014021.	2.1	64
24	Cryogenic tritium-hydrogen-deuterium and deuterium-tritium layer implosions with high density carbon ablators in near-vacuum hohlraums. Physics of Plasmas, 2015, 22, 062703.	1.9	62
25	Measurements of an Ablator-Gas Atomic Mix in Indirectly Driven Implosions at the National Ignition Facility. Physical Review Letters, 2014, 112, 025002.	7.8	60
26	Hohlraum energetics scaling to 520 TW on the National Ignition Facility. Physics of Plasmas, 2013, 20, .	1.9	59
27	Energy penetration into arrays of aligned nanowires irradiated with relativistic intensities: Scaling to terabar pressures. Science Advances, 2017, 3, e1601558.	10.3	58
28	Imaging of high-energy x-ray emission from cryogenic thermonuclear fuel implosions on the NIF. Review of Scientific Instruments, 2012, 83, 10E115.	1.3	57
29	Assembly of High-Areal-Density Deuterium-Tritium Fuel from Indirectly Driven Cryogenic Implosions. Physical Review Letters, 2012, 108, 215005.	7.8	57
30	Thin Shell, High Velocity Inertial Confinement Fusion Implosions on the National Ignition Facility. Physical Review Letters, 2015, 114, 145004.	7.8	56
31	Achieving record hot spot energies with large HDC implosions on NIF in HYBRID-E. Physics of Plasmas, 2021, 28, .	1.9	55
32	X-ray driven implosions at ignition relevant velocities on the National Ignition Facility. Physics of Plasmas, 2013, 20, .	1.9	54
33	2015, 22, 056314.	1.9	49
34	The role of hot spot mix in the low-foot and high-foot implosions on the NIF. Physics of Plasmas, 2017, 24, .	1.9	49
35	Performance of High-Convergence, Layered DT Implosions with Extended-Duration Pulses at the National Ignition Facility. Physical Review Letters, 2013, 111, 215001.	7.8	47
36	Dynamic high energy density plasma environments at the National Ignition Facility for nuclear science research. Journal of Physics G: Nuclear and Particle Physics, 2018, 45, 033003.	3.6	47

#	Article	IF	CITATIONS
37	High-energy (>70 keV) x-ray conversion efficiency measurement on the ARC laser at the National Ignition Facility. Physics of Plasmas, 2017, 24, .	1.9	45
38	Early-Time Symmetry Tuning in the Presence of Cross-Beam Energy Transfer in ICF Experiments on the National Ignition Facility. Physical Review Letters, 2013, 111, 235001.	7.8	44
39	Multispectral x-ray imaging with a pinhole array and a flat Bragg mirror. Review of Scientific Instruments, 2005, 76, 073708.	1.3	42
40	Making relativistic positrons using ultraintense short pulse lasers. Physics of Plasmas, 2009, 16, 122702.	1.9	42
41	Development of the CD Symcap platform to study gas-shell mix in implosions at the National Ignition Facility. Physics of Plasmas, 2014, 21, .	1.9	42
42	Short pulse, high resolution, backlighters for point projection high-energy radiography at the National Ignition Facility. Physics of Plasmas, 2017, 24, .	1.9	42
43	Increasing stagnation pressure and thermonuclear performance of inertial confinement fusion capsules by the introduction of a high-Z dopant. Physics of Plasmas, 2018, 25, .	1.9	42
44	Development of backlighting sources for a Compton radiography diagnostic of inertial confinement fusion targets (invited). Review of Scientific Instruments, 2008, 79, 10E901.	1.3	41
45	Saturation in a Ni-like Pd soft-x-ray laser at 14.7 nm. Physical Review A, 1999, 59, 1577-1581.	2.5	39
46	Extracting core shape from x-ray images at the National Ignition Facility. Review of Scientific Instruments, 2012, 83, 10E519.	1.3	39
47	Absolute Equation-of-State Measurement for Polystyrene from 25 to 60ÂMbar Using a Spherically Converging Shock Wave. Physical Review Letters, 2018, 121, 025001.	7.8	39
48	High-density carbon capsule experiments on the national ignition facility. Physical Review E, 2015, 91, 021101.	2.1	38
49	Performance of indirectly driven capsule implosions on the National Ignition Facility using adiabat-shaping. Physics of Plasmas, 2016, 23, 056303.	1.9	38
50	The scaling of electron and positron generation in intense laser-solid interactions. Physics of Plasmas, 2015, 22, .	1.9	37
51	First beryllium capsule implosions on the National Ignition Facility. Physics of Plasmas, 2016, 23, 056310.	1.9	37
52	Towards laboratory produced relativistic electron–positron pair plasmas. High Energy Density Physics, 2011, 7, 225-229.	1.5	36
53	K-shell spectra from Ag, Sn, Sm, Ta, and Au generated by intense femtosecond laser pulses. High Energy Density Physics, 2007, 3, 263-271.	1.5	35
54	Progress towards ignition on the National Ignition Facility. Nuclear Fusion, 2011, 51, 094024.	3.5	35

Riccardo Tommasini

#	Article	IF	CITATIONS
55	A novel tape target for use with repetitively pulsed lasers. Review of Scientific Instruments, 2002, 73, 2190-2192.	1.3	33
56	Frequency doubling of multi-terawatt femtosecond pulses. Applied Physics B: Lasers and Optics, 2004, 79, 547-554.	2.2	33
57	Symmetry tuning of a near one-dimensional 2-shock platform for code validation at the National Ignition Facility. Physics of Plasmas, 2016, 23, .	1.9	33
58	Enhanced energy coupling for indirectly driven inertial confinement fusion. Nature Physics, 2019, 15, 138-141.	16.7	32
59	Bremsstrahlung hard x-ray source driven by an electron beam from a self-modulated laser wakefield accelerator. Plasma Physics and Controlled Fusion, 2018, 60, 054008.	2.1	31
60	Spectroscopic determination of temperature and density spatial profiles and mix in indirect-drive implosion cores. Physical Review E, 2007, 76, 056403.	2.1	28
61	Simulations and experiments of the growth of the "tent―perturbation in NIF ignition implosions. Journal of Physics: Conference Series, 2016, 717, 012021.	0.4	28
62	Experimental results of radiation-driven, layered deuterium-tritium implosions with adiabat-shaped drives at the National Ignition Facility. Physics of Plasmas, 2016, 23, .	1.9	27
63	Time-Resolved Fuel Density Profiles of the Stagnation Phase of Indirect-Drive Inertial Confinement Implosions. Physical Review Letters, 2020, 125, 155003.	7.8	27
64	Emittance of positron beams produced in intense laser plasma interaction. Physics of Plasmas, 2013, 20, .	1.9	26
65	Investigation of a polychromatic tomography method for the extraction of the three-dimensional spatial structure of implosion core plasmas. Physics of Plasmas, 2012, 19, 082705.	1.9	25
66	Direct asymmetry measurement of temperature and density spatial distributions in inertial confinement fusion plasmas from pinhole space-resolved spectra. Physics of Plasmas, 2014, 21, .	1.9	25
67	Ultra-high (>30%) coupling efficiency designs for demonstrating central hot-spot ignition on the National Ignition Facility using a Frustraum. Physics of Plasmas, 2019, 26, .	1.9	25
68	In-flight observations of low-mode <i>Ï</i> R asymmetries in NIF implosions. Physics of Plasmas, 2015, 22,	1.9	24
69	Measurements of core and compressed-shell temperature and density conditions in thick-wall target implosions at the OMEGA laser facility. Physical Review E, 2011, 83, 066408.	2.1	23
70	Measurement of electron temperature of imploded capsules at the National Ignition Facility. Review of Scientific Instruments, 2012, 83, 10E121.	1.3	23
71	X-ray sources using a picosecond laser driven plasma accelerator. Physics of Plasmas, 2019, 26, .	1.9	22
72	Experimental study of neutron induced background noise on gated x-ray framing cameras. Review of Scientific Instruments, 2010, 81, 10E515.	1.3	21

#	Article	IF	CITATIONS
73	Processing of spectrally resolved x-ray images of inertial confinement fusion implosion cores recorded with multimonochromatic x-ray imagers. Journal of Applied Physics, 2011, 109, .	2.5	21
74	Mix and hydrodynamic instabilities on NIF. Journal of Instrumentation, 2017, 12, C06001-C06001.	1.2	21
75	Comparison of genetic-algorithm and emissivity-ratio analyses of image data from OMEGA implosion cores. Review of Scientific Instruments, 2008, 79, 10E921.	1.3	20
76	Analysis of time-resolved argon line spectra from OMEGA direct-drive implosions. Review of Scientific Instruments, 2008, 79, 10E310.	1.3	20
77	Tests and calibration of NIF neutron time of flight detectors. Review of Scientific Instruments, 2008, 79, 10E527.	1.3	20
78	Argon K-shell and bound-free emission from OMEGA direct-drive implosion cores. High Energy Density Physics, 2010, 6, 70-75.	1.5	20
79	The effect of shock dynamics on compressibility of ignition-scale National Ignition Facility implosions. Physics of Plasmas, 2014, 21, .	1.9	20
80	A near one-dimensional indirectly driven implosion at convergence ratio 30. Physics of Plasmas, 2018, 25, .	1.9	20
81	Achieving 280 Gbar hot spot pressure in DT-layered CH capsule implosions at the National Ignition Facility. Physics of Plasmas, 2020, 27, .	1.9	20
82	Enhanced laser–plasma interactions using non-imaging optical concentrator targets. Optica, 2020, 7, 129.	9.3	20
83	Application of fall-line mix models to understand degraded yield. Physics of Plasmas, 2008, 15, .	1.9	18
84	Multispectral x-ray imaging for core temperature and density maps retrieval in direct drive implosions. Review of Scientific Instruments, 2006, 77, 10E303.	1.3	17
85	Development of two mix model postprocessors for the investigation of shell mix in indirect drive implosion cores. Physics of Plasmas, 2007, 14, 072705.	1.9	17
86	Radiative shocks produced from spherical cryogenic implosions at the National Ignition Facility. Physics of Plasmas, 2013, 20, 056315.	1.9	17
87	First demonstration of improved capsule implosions by reducing radiation preheat in uranium vs gold hohlraums. Physics of Plasmas, 2018, 25, .	1.9	17
88	Single-shot measurement of laser-induced damage thresholds of thin film coatings. Optics Communications, 1998, 152, 168-174.	2.1	15
89	Generation of monoenergetic ultrashort electron pulses from a fs laser plasma. Applied Physics B: Lasers and Optics, 2004, 79, 923-926.	2.2	15
90	Development of Compton radiography using high-Z backlighters produced by ultra-intense lasers. AIP Conference Proceedings, 2007, , .	0.4	15

#	Article	IF	CITATIONS
91	Inference of ICF implosion core mix using experimental dataand theoretical mix modeling. High Energy Density Physics, 2009, 5, 249-257.	1.5	15
92	Development of new platforms for hydrodynamic instability and asymmetry measurements in deceleration phase of indirectly driven implosions on NIF. Physics of Plasmas, 2018, 25, 082705.	1.9	15
93	Exploring implosion designs for increased compression on the National Ignition Facility using high density carbon ablators. Physics of Plasmas, 2022, 29, .	1.9	15
94	Iterative method for phase-amplitude retrieval and its application to the problem of beam-shaping and apodization. Optics Communications, 1998, 153, 339-346.	2.1	14
95	Core temperature and density profile measurements in inertial confinement fusion implosions. High Energy Density Physics, 2008, 4, 1-17.	1.5	14
96	Performance of beryllium targets with full-scale capsules in low-fill 6.72-mm hohlraums on the National Ignition Facility. Physics of Plasmas, 2017, 24, .	1.9	14
97	Compensation of nonlinear self-focusing in high-power lasers. IEEE Journal of Quantum Electronics, 2000, 36, 687-691.	1.9	13
98	Reconstruction of 2D x-ray radiographs at the National Ignition Facility using pinhole tomography (invited). Review of Scientific Instruments, 2014, 85, 11E503.	1.3	13
99	Excitation-velocity and group-velocity mismatch in amplified spontaneous emission lasers: A discussion on the transient gain x-ray lasers. Physical Review A, 2000, 62, .	2.5	12
100	Limits on collective X-ray scattering imposed by coherence. Europhysics Letters, 2006, 74, 637-643.	2.0	12
101	Beam and target alignment at the National Ignition Facility using the Target Alignment Sensor (TAS). Proceedings of SPIE, 2012, , .	0.8	12
102	Simulations of indirectly driven gas-filled capsules at the National Ignition Facility. Physics of Plasmas, 2014, 21, .	1.9	12
103	Time-resolved characterization and energy balance analysis of implosion core in shock-ignition experiments at OMEGA. Physics of Plasmas, 2014, 21, .	1.9	12
104	Amplified spontaneous emission and maximum gain–length product revised for general line shapes. Journal of the Optical Society of America B: Optical Physics, 1999, 16, 538.	2.1	11
105	High-energy differential-filtering photon spectrometer for ultraintense laser-matter interactions. Review of Scientific Instruments, 2018, 89, 10F116.	1.3	11
106	Coherence properties of an amplified spontaneous emission laser: experiments on a 10 Hz vacuum–ultraviolet H2-laser. Optics Communications, 2000, 180, 277-283.	2.1	10
107	<title>Investigations on 10-Hz sub-Joule fs-laser pumped neon- and nickel-like x-ray lasers</title> . , 2001, , .		10
108	Preplasma conditions for operation of10â^'Hzsubjoule femtosecond-laser-pumped nickel-like x-ray lasers. Physical Review E, 2004, 69, 066404.	2.1	10

#	Article	IF	CITATIONS
109	Diffraction of laser-plasma-generated electron pulses. Applied Physics B: Lasers and Optics, 2005, 81, 155-157.	2.2	10
110	Applied plasma spectroscopy: Laser-fusion experiments. High Energy Density Physics, 2009, 5, 234-243.	1.5	10
111	Assessment and mitigation of radiation, EMP, debris & shrapnel impacts at megajoule-class laser facilities. Journal of Physics: Conference Series, 2010, 244, 032018.	0.4	10
112	AXIS: An instrument for imaging Compton radiographs using the Advanced Radiography Capability on the NIF. Review of Scientific Instruments, 2014, 85, 11D624.	1.3	10
113	Spectroscopic modeling of an argon-doped shock-ignition implosion. Review of Scientific Instruments, 2010, 81, 10E307.	1.3	9
114	Advanced gated x-ray imagers for experiments at the National Ignition Facility. Proceedings of SPIE, 2011, , .	0.8	9
115	Measuring electron-positron annihilation radiation from laser plasma interactions. Review of Scientific Instruments, 2012, 83, 10E113.	1.3	9
116	Numerical simulation of thin-shell direct drive DHe3-filled capsules fielded at OMEGA. Physics of Plasmas, 2012, 19, .	1.9	9
117	Capsule Ablator Inflight Performance Measurements Via Streaked Radiography Of ICF Implosions On The NIF*. Journal of Physics: Conference Series, 2016, 688, 012014.	0.4	9
118	Shell stability and conditions analyzed using a new method of extracting shell areal density maps from spectrally resolved images of direct-drive inertial confinement fusion implosions. Physics of Plasmas, 2016, 23, .	1.9	9
119	Observation of saturated lasing on the 3p–3s, J=0–1 transition at 25.5 nm in neon-like iron using a double-prepulse technique. Optics Communications, 1998, 154, 325-328.	2.1	8
120	Saturation in neon- and nickel-like collisional soft-X-ray lasers at low pump energy. IEEE Journal of Selected Topics in Quantum Electronics, 1999, 5, 1435-1440.	2.9	8
121	Soft-x-ray lasing and saturation in nickellike silver at pump energies below 30 J. Journal of the Optical Society of America B: Optical Physics, 1999, 16, 1664.	2.1	8
122	Generalized Linford formula. Journal of the Optical Society of America B: Optical Physics, 2000, 17, 1665.	2.1	8
123	Effective traveling-wave excitation below the speed of light. Optics Letters, 2001, 26, 689.	3.3	8
124	Development of spectroscopic tools for the determination of temperature and density spatial profiles in implosion cores. High Energy Density Physics, 2007, 3, 287-291.	1.5	8
125	Development of a dual MCP framing camera for high energy x-rays. Review of Scientific Instruments, 2014, 85, 11D623.	1.3	8
126	Multiobjective method for fitting pinhole image intensity profiles of implosion cores driven by a Pareto genetic algorithm. Review of Scientific Instruments, 2006, 77, 10F525.	1.3	7

#	Article	IF	CITATIONS
127	Spatial structure analysis of direct-drive implosion cores at OMEGA using x-ray narrow-band core images. Review of Scientific Instruments, 2006, 77, 10E320.	1.3	7
128	Absolute laser energy absorption measurement of relativistic 0.7 ps laser pulses in nanowire arrays. Physics of Plasmas, 2021, 28, .	1.9	7
129	Summary of the first neutron image data collected at the National Ignition Facility. EPJ Web of Conferences, 2013, 59, 13017.	0.3	6
130	Automated analysis of hot spot X-ray images at the National Ignition Facility. Review of Scientific Instruments, 2016, 87, 11E334.	1.3	6
131	Using a 2-shock 1D platform at NIF to measure the effect of convergence on mix and symmetry. Physics of Plasmas, 2018, 25, 102702.	1.9	6
132	Efficient J=0-1 soft-X-ray lasing in neon-like ions at pump powers below 250ÂGW. Applied Physics B: Lasers and Optics, 1998, 66, 561-566.	2.2	5
133	VUV laser in the Lyman band of molecular hydrogen pumped by fs titanium-sapphire laser pulses. IEEE Journal of Selected Topics in Quantum Electronics, 1999, 5, 1510-1514.	2.9	5
134	X-ray imaging in an environment with high-neutron background on National Ignition Facility. , 2011, , .		5
135	Understanding reliability and some limitations of the images and spectra reconstructed from a multi-monochromatic x-ray imager. Review of Scientific Instruments, 2015, 86, 113505.	1.3	5
136	Symmetry tuning and high energy coupling for an Al capsule in a Au rugby hohlraum on NIF. Physics of Plasmas, 2020, 27, .	1.9	5
137	Narrow-band x-ray imaging for core temperature and density maps retrieval of direct drive implosions. , 2006, , .		4
138	High energy x-ray imager for inertial confinement fusion at the National Ignition Facility. Review of Scientific Instruments, 2006, 77, 10E301.	1.3	4
139	Experimental evaluation of neutron induced noise on gated x-ray framing cameras. Journal of Physics: Conference Series, 2010, 244, 032048.	0.4	4
140	K-shell spectroscopy of Au plasma generated with a short-pulse laser <sup>1</sup> This article is part of a Special Issue on the 10th International Colloquium on Atomic Spectra and Oscillator Strengths for Astrophysical and Laboratory Plasmas Canadian Journal of Physics, 2011, 89, 647-651.	1.1	4
141	An important criterion for reliable multi-monochromatic x-ray imager diagnostics and its impact on the reconstructed images. High Power Laser Science and Engineering, 2015, 3, .	4.6	4
142	Hydroscaling indirect-drive implosions on the National Ignition Facility. Physics of Plasmas, 2022, 29, .	1.9	4
143	Generation of Attosecond X-Ray Laser Pulses. IEEE Journal of Selected Topics in Quantum Electronics, 2004, 10, 1388-1392.	2.9	3
144	Convergent-beam diffraction of ultra-short hard X-ray pulses focused by a capillary lens. Applied Physics B: Lasers and Optics, 2006, 82, 519-522.	2.2	3

#	Article	IF	CITATIONS
145	Hydrodynamic instabilities and mix studies on NIF: predictions, observations, and a path forward. Journal of Physics: Conference Series, 2016, 688, 012090.	0.4	3
146	X-ray drive of beryllium capsule implosions at the National Ignition Facility. Journal of Physics: Conference Series, 2016, 717, 012058.	0.4	3
147	Spatial resolution measurements of the advanced radiographic capability x-ray imaging system at energies relevant to Compton radiography. Review of Scientific Instruments, 2016, 87, 11E310.	1.3	3
148	Absorption of relativistic multi-picosecond laser pulses in wire arrays. Physics of Plasmas, 2021, 28, 103102.	1.9	3
149	Focusing and collimation of laser-generated ultrashort x-ray pulses by polycapillary lenses. , 2005, , .		2
150	Recovery of a chemical vapor deposited diamond detection system from strong pulses of laser produced x rays. Review of Scientific Instruments, 2006, 77, 10F316.	1.3	2
151	Comparing neutron and X-ray images from NIF implosions. EPJ Web of Conferences, 2013, 59, 04002.	0.3	2
152	Control of Be capsule low mode implosions symmetry at the National Ignition Facility. Journal of Physics: Conference Series, 2016, 717, 012033.	0.4	2
153	Use of 41Ar production to measure ablator areal density in NIF beryllium implosions. Physics of Plasmas, 2017, 24, .	1.9	2
154	A dual high-energy radiography platform with 15 μm resolution at the National Ignition Facility. Review of Scientific Instruments, 2021, 92, 043712.	1.3	2
155	Saturated lasing in neon- and nickel-like ions at pump energies below 30 J. , 1999, , .		1
156	Analysis of the visible emission from optical-field–ionized hydrogen. Europhysics Letters, 2000, 49, 27-33.	2.0	1
157	Ultrafast x-ray diffraction studies on Si(111) and DMABN crystals using Cu-K-α radiation. , 2004, 5196, 311.		1
158	Deposition and analysis of small d-spacing depth graded multilayer structures. Proceedings of SPIE, 2007, , .	0.8	1
159	Four-objective analysis including an optically thick line to extract electron temperature and density profiles in ICF implosion cores. Journal of Physics: Conference Series, 2008, 112, 022014.	0.4	1
160	Gamma background calculation for the HEXRI diagnostic at the National Ignition Facility. Journal of Physics: Conference Series, 2008, 112, 032085.	0.4	1
161	Ignition X-ray imager for laser-fusion research at the national ignition facility. European Physical Journal Special Topics, 2006, 133, 935-937.	0.2	1
162	Preplasma conditions for the operation of 10-Hz sub-Joule fs-laser-pumped nickel-like x-ray lasers. , 2003, , .		0

#	Article	IF	CITATIONS
163	Attosecond x-ray laser pulses. , 2005, , .		0
164	Electron Diffraction Experiments using Laser Plasma Electrons. AIP Conference Proceedings, 2006, , .	0.4	0
165	Spectroscopic study of temperature and density spatial profiles and mix in implosion cores. , 2008, , .		0
166	Using x-rays to test chemical vapor deposited diamond detectors for areal density measurement at the National Ignition Facility. Review of Scientific Instruments, 2008, 79, 10E931.	1.3	0
167	Core temperature and shape measurements from ignition implosions at the National Ignition Facility using multispectral x-ray imaging. , 2009, , .		0
168	Non-Equilibrium Electron And Ion Temperature Measurements In Omega Direct-Drive Implosions. , 2009, , .		0
169	Intrinsic fast neutron sensitivity of imaging plates. , 2009, , .		0
170	Hard x-ray spectrometer for hot electron measurements on the National Ignition Facility. , 2009, , .		0
171	Simulation of radiation backgrounds associated with the HEXRI diagnostics at the National Ignition Facility. Journal of Physics: Conference Series, 2010, 244, 032049.	0.4	0
172	Demonstration of enhanced DQE with a dual MCP configuration. , 2014, , .		0
173	Overview of Performance and Progress with Inertially Confined Fusion Implosions on the National Ignition Facility. , 2015, , .		0
174	Getting Beyond Unity Fusion Fuel Gain in an Inertially Confined Fusion Implosion. , 2015, , .		0
175	Performance of indirectly driven capsule implosions on NIF using adiabat-shaping. Journal of Physics: Conference Series, 2016, 717, 012045.	0.4	0
176	Temporal evolution of the two-shock implosion on the National Ignition Facility. , 2016, , .		0
177	Generalized Linford formula and its application to Traveling Wave Excitation. European Physical Journal Special Topics, 2001, 11, Pr2-285-Pr2-288.	0.2	0
178	Underdense radiation sources: Moving towards longer wavelengths. European Physical Journal Special Topics, 2006, 133, 1173-1175.	0.2	0
179	An Attempt to Generate an Inner-Shell Photo-Ionisation Pumped X-Ray Laser Using the ASTRA Laser at RAL. Springer Proceedings in Physics, 2009, , 537-542.	0.2	0